Brain connectivity, Dynamics and Cognition Lab
School of Artificical Intelligence and Data Science
Indian Institute of Technology, Jodhpur

SAIDE SUMMER INTERNSHIP PROJECT REPORT

Uncertainty Representation Plays a Major Role in Emotional Dynamics

linked to the project

Age related changes in representation of uncertainty leads to differential emotion perception

Rishi Dey Chowdhury

Indian Statistical Institute, Kolkata

Bachelor of Statistics

Program Joining Date: May, 2022

Dr. Dipanjan Roy

Gargi Majumdar (PhD)

SUMMARY

INTRODUCTION

Understanding the dynamics of our affective experiences has been one of the hardest problems in the field of neuroscience owing to the complexity of the phenomenon. Prevalent theories have mainly tried to characterize emotions using two dimensions of Arousal and Valence. However, empirical works have shown that these are insufficient in explaining real-life complexity and dynamicity of our affective experiences. In this domain, an unresolved question that still exists is how these emotional experiences change with age. Basing our work on a previous study which showed uncertainty to be a central parameter in mediating affective dynamics, we tried to explain the differential emotional experience in older individuals from a representational and computational level, using unsupervised approaches and sophisticated neural network models.

OBJECTIVE

In the past, emotions are understood as a combination of two measures of Valence and Arousal. Hence, analysis or work on emotions previously meant collecting data on these two variables for each individual. But as per the recent work by Majumdar et. al., it proposes that uncertainty plays an important role in explaining the emotional dynamics. Hence, the objective of our study is to explore this hypothesis as well as trying to come up with a quantification of uncertainty.
Another major objective of the study is to compare the emotional response between young and old subjects based on the significant difference in uncertainty processing. So, we hypothesize that the lack of uncertainty representation might be the reason of difference in emotions exhibited by young and old subjects. Hence, another goal of our study is to find a sufficient method for uncertainty representation.
Although both the above goals might be similar, the first one deals with quantitative analysis of uncertainty whereas the second one maybe a visual representation.

DATA

Stimulus. In our study we analyzed the behavioral data of participants on a Facial recognition task where they were presented with different faces portraying either of the 6 basic emotions – Happy, Sad, Anger, Fear, Disgust and Surprise.
For the neural analyses we examined the neuroimaging responses of participants to a tailored version (8mins) of a black-and-white movie by Alfred Hitchcock called “Bang! You’re Dead!” which we divided into several emotionally dynamic scenes – Ascent (high intense), Descent (low intense) and Control.

Participants. A total of 209 participants were selected from the healthy population derived CamCAN cohort. The participants were grouped into Young (18-35 years, Mean age:27.5) and Old (60-88 years, Mean age: 70).

Neuroimaging Data. After preprocessing the fMRI (functional Magnetic Resonance Imaging) data, we extracted the BOLD (Blood Oxygen Level Dependent) timeseries for all participants for this movie watching task. The first 4 scans were removed results in a total of 189 timepoints (TR) for each participant. We extracted data at both ROI (Region of Interest) and voxel level.
The final pre-processed data of the i^{th} subject for the j^{th} ROI, let us denote by $X_j^{(i)}$ is of the shape $TRs \times Voxs$, where TRs refer to the total number of time points(each captured at an interval of

2.47 seconds) which is 189 and $Voxs$ refer to the total number of voxels in the j^{th} ROI.

METHODOLOGY

For the representational level we wanted to explore the low dimensional manifolds for representation of uncertainty in Young and Old using few data driven analyses.

Dimension Reduction. Dimension Reduction is a well-known technique for feature extraction and data-visualization of high-dimensional data. In our case, we want to extract low-dimensional signature or pattern of the averaged data $\bar{X_j} = \frac{\Sigma_{i=1}^{n} X_j^{(i)}}{111}$, where n is the number of subjects, for each j^{th} ROI corresponding to the young and the old subjects for the sake of comparison and find out the ROIs which differs the most and might be responsible for uncertainty processing as hinted and analyzed to some extent before. We carried out the following Dimension Reduction techniques:

- Principle Component Analysis(PCA)
- t-Distributed Stochastic Neighbor Embedding (t-SNE)
- Potential of Heat-diffusion for Affinity-based Trajectory Embedding(PHATE)
- Temporal Potential of Heat-diffusion for Affinity-based Trajectory Embedding(TPHATE)

Principle Component Analysis. The principal components of a collection of points in a real coordinate space are a sequence of p unit vectors, where the i^{th} is the direction of a line that best fits the data while being orthogonal to the first $i - 1$ vectors. Here, a best-fitting line is defined as one that minimizes the average squared distance from the points to the line. These directions constitute an orthonormal basis in which different individual dimensions of the data are linearly uncorrelated. PCA is the process of computing the principal components and using them to perform a change of basis on the data, sometimes using only the first few principal components and ignoring the rest.
The PCA algorithm works by finding the eigenvalues and eigenvectors of the data matrix using Singular Value Decomposition(SVD) and then ordering the eigenvectors in descending order based on the eigenvalues and then picking up first few eigenvectors as the basis and reconstructing the data back by using these new loading vectors. Eigenvalues give the idea about the strength or variance explained.
In our case we applied PCA on the matrix $\bar{X_j}$ for young and old separately for each j^{th} ROI. PCA is an algorithm which looks at the overall direction of the data to pick up orthogonal directions that explains the variance in the data the most. Apart from just the direction it also sheds light on the magnitude of the strength of the variance explained by each direction. In our case this has the effect of capturing the overall spatial spread of the data in the first two directions which are responsible for explaining majority of the variance and compare the results for young and old. Magnitude of the variance explained gives interesting results for comparing the old and young subject's ROIs.
PCA captures the overall global relationship in the data at the cost of shattering local information, like proximity of two points or similar characteristics.

t-Distributed Stochastic Neighbor Embedding. t-SNE is a statistical method for visualizing high-dimensional data by giving each datapoint a location in a two or three-dimensional map. It is a nonlinear dimensionality reduction technique well-suited for embedding high-dimensional data for visualization in a low-dimensional space of two or three dimensions. Specifically, it models each high-dimensional object by a two- or three-dimensional point in such a way that

similar objects are modeled by nearby points and dissimilar objects are modeled by distant points with high probability.
The t-SNE algorithm comprises two main stages. First, t-SNE constructs a probability distribution over pairs of high-dimensional objects in such a way that similar objects are assigned a higher probability while dissimilar points are assigned a lower probability. Second, t-SNE defines a similar probability distribution over the points in the low-dimensional map, and it minimizes the Kullback–Leibler divergence (KL divergence) between the two distributions with respect to the locations of the points in the map.
In our case we applied PCA on the matrix $\bar{X}_j$ for young and old separately for each j^{th} ROI. t-SNE is primarily a high-dimensional data visualization technique. It sacrifices the global relationship in the data at the cost of preserving local information. We use it to compare how close are the local behavior of the young subject's ROI to the old subject's ROI.

Potential of Heat-diffusion for Affinity-based Trajectory Embedding. PHATE provides a denoised, two or three-dimensional visualization of the complete branching trajectory structure in high-dimensional data. It uses heat-diffusion processes, which naturally denoise the data, to compute data point affinities. Then, PHATE creates a diffusion-potential geometry by free-energy potentials of these processes. This geometry captures high-dimensional trajectory structures, while enabling a natural embedding of the intrinsic data geometry. This embedding accurately visualizes trajectories and data distances, without requiring strict assumptions typically used by path-finding and tree-fitting algorithms, which have recently been used for pseudotime orderings or tree-renderings of high dimensional data with hierarchy.
Given a dataset of voxel time-series data, $\bar{X}_j$. Construction of the PHATE diffusion geometry starts by computing the Euclidean distance matrix D between data pairs, where $D(i, j) = ||X_{i,} - X_{j,}||_2$. D is then converted into a local affinity matrix K using an adaptive bandwidth Gaussian kernel. The affinity matrix K is then row-normalized to get the initial probabilities P_D, which are used for the Markovian random-walk diffusion process.The diffusion operator P_D is then raised to the t_D^{th} power, where t_D is the PHATE optimal diffusion time scale, to perform a t_D-step random walk over the data graph. This specific diffusion process infers more global relations beyond the local affinities. To further preserve both local and manifold-intrinsic global structure of data, PHATE computes the diffusion potential U by taking the logarithm of P_D^{tD} and the diffusion potential distance D_U using distance between row pairs of U. This diffusion potential distance can be reduced to $2 - 3$ dimensions for visualization or to any other dimensionality (such as that obtained by cross-validation) by performing metric MDS (MMDS).

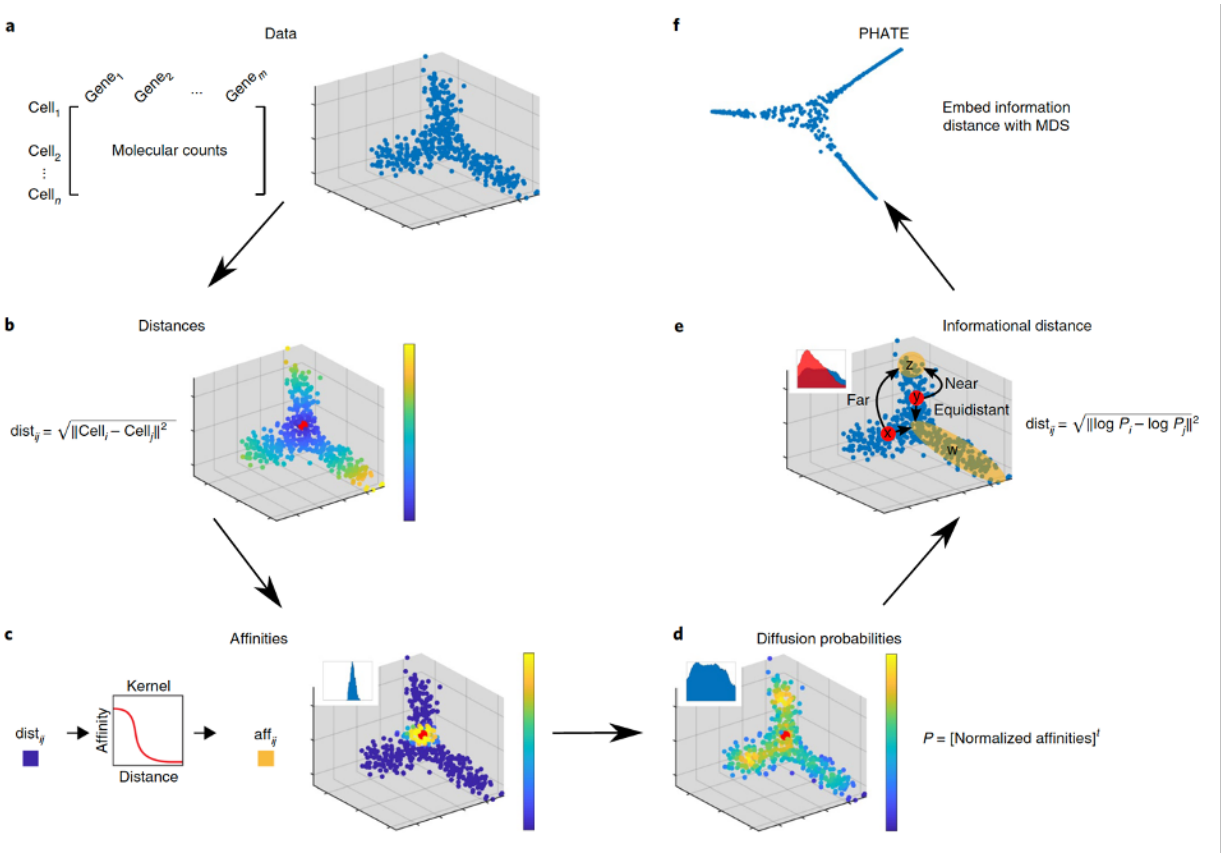

Figure 1. Moon et al., Nature Biotechnology 2019, Visualizing structure and transitions in high-dimensional biological data

In our case we applied PCA on the matrix $\bar{X}_j$ for young and old separately for each j^{th} ROI. It better captured the closeness between the datapoints wrt vicinity as well as temporal vicinity.

Temporal Potential of Heat-diffusion for Affinity-based Trajectory Embedding. TPHATE is a modified PHATE algorithm which is able to capture the temporal aspect of the data. The algorithm works the same as original PHATE except for the temporal component infused in the diffusion matrix using the auto-covariance function in a Temporal Affinity Matrix, which is explained below.

TPHATE as a variant of PHATE that uses a dual-view diffusion operator to embed timeseries data in a low-dimensional space. The first view, P_D, of the diffusion operator uses the same process as PHATE to build an affinity matrix based on the Euclidean distance between data samples (here, timepoints) and then row-normalize it to obtain the transition probability matrix, where PD is a TxT matrix. The second view P_T is based on an affinity matrix that summarizes the autocorrelation function of the data. First we calculate a direct estimator of the autocovariance of the timeseries vector V from each voxel using $|V|1$ lags. Then the functions are averaged across voxels to obtain a single autocorrelation function (acf) and smoothed with a rolling average over w timepoints, to account for possible jittering around where $acf = 0$. Next, we find the first lag $lagmax$ where $acf = 0$, which defines the maximum width of smoothing for the temporal affinity matrix A. The temporal affinity matrix A is calculated as $A(i, j) = acf(i, j), 0 < |ij| \leq lagmax$ and 0 elsewhere. The autocorrelative probability P_t is obtained by row-normalizing the affinity matrix A. These views are combined with alternating diffusion into a single operator $P = P_D P_T$, which is used as the initial probabilities for diffusion. The rest of constructing diffusion geometry

and data visualization is performed the same as in PHATE. This dual-view diffusion step allows T-PHATE to learn data geometry and latent signals that represent cognitive processes that play out over longer temporal windows.

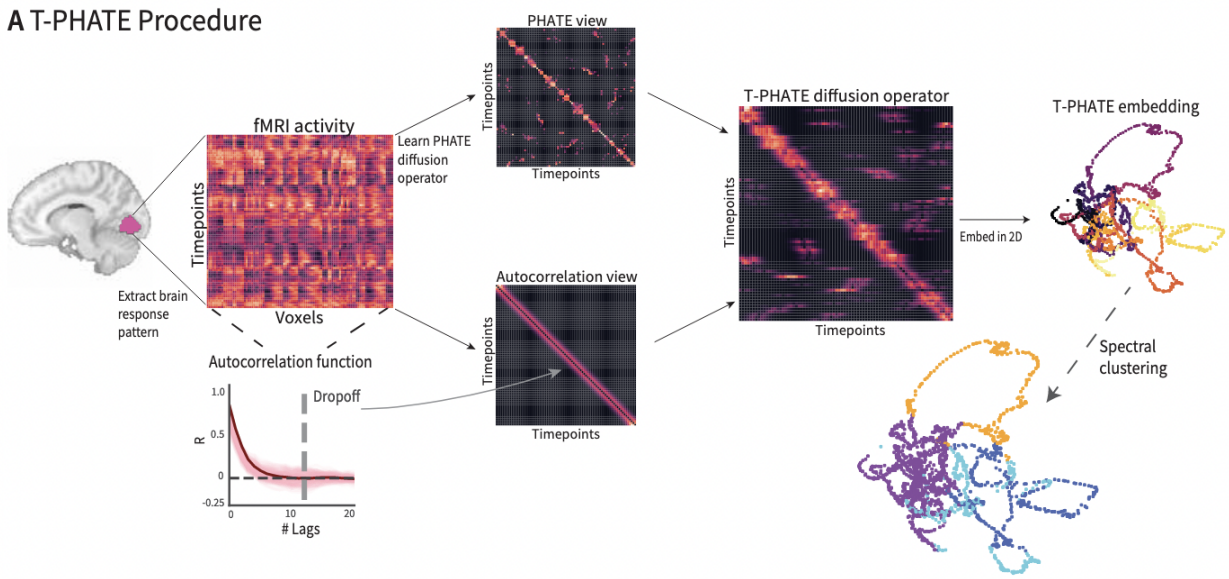

Figure 2. Busch et al., TPHATE Algorithm Visualized taken from Temporal PHATE: A multi-view manifold learning method for brain state trajectories

It is suited to be applied in the context of High-Dimensional(Number of Voxels) BOLD time series i.e. the matrix $\bar{X}_j$ for young and old separately for each j^{th} ROI.

Sequence Modelling. Sequence Modeling is the technique of training models on data that has a temporal component associated with it to predict the next value/state. Realizing that our data matrix $\bar{X}_j$ for young and old for each of the j^{th} ROI has a time axis. We looked forward to train sequence models to capture an approximation of the uncertainty information in our model(since, our model will learn to predict the BOLD values given the previous BOLD values). If the predictions are accurate then it will imply we have captured the uncertainty associated with the movie watching data and hence, can be used for quantifying the uncertainty. But there lies several difficulties and challenges to overcome for the model to successfully capture this information. We focused on the following models for our analysis:

- Long Short-Term Memory Neural Network(LSTM)

Long Short-Term Memory Neural Network. LSTMs are better than Recurrent Neural Networks(RNN) at carrying information from past time steps to farther time steps ahead and improves gradient update values preventing issues like vanishing or exploding gradients which is an issue with RNNs.
LSTM unit has a memory cell and three gates: input gate, output gate and forget gate. Intuitively, at time step t, the input gate i_t controls how much each unit is updated, the output gate o_t controls the exposure of the internal memory state, and the forget gate f_t controls the amount of which each unit of the memory cell is erased. The memory cell c_t keeps the useful history information which will be used for the next process.
Mathematically, the states of LSTM are updated as follows:

$$i_t = \sigma(W_{xi}x_t + W_{hi}h_{t-1} + W_{ci}c_{t-1} + b_i)$$

$$
\begin{aligned}
f_t &= \sigma(W_{xf}x_t + W_{hf}h_{t-1} + W_{cf}c_{t-1} + b_f) \\
f_o &= \sigma(W_{xo}x_t + W_{ho}h_{t-1} + W_{co}c_{t-1} + b_o) \\
c_t &= f_t \odot c_{t-1} + i_t \odot \tanh(W_{xc}x_t + W_{hc}h_{t-1} + b_c) \\
h_t &= o_t \odot \tanh(c_t)
\end{aligned}
$$

where x_t is the input vector at the current time step, σ denotes the logistic sigmoid function and $\odot$ denotes elementwise multiplication. Note that W_{ci}, W_{cf} and W_{co} are weight matrices.
For prediction at each time step we pass the hidden state h_t to a fully connected NN with ReLU activation except for the last layer, which can be represented mathematically as follows:

$$
\begin{aligned}
\hat{x}_{t+1} &= W_i h_t \\
\hat{x}_{t+1} &= relu(\hat{x}_{t+1}) \\
&\dots \\
\hat{x}_{t+1} &= W_N \hat{x_{t+1}}
\end{aligned}
$$

where $i = 1, \dots N$ is the dense layer number.

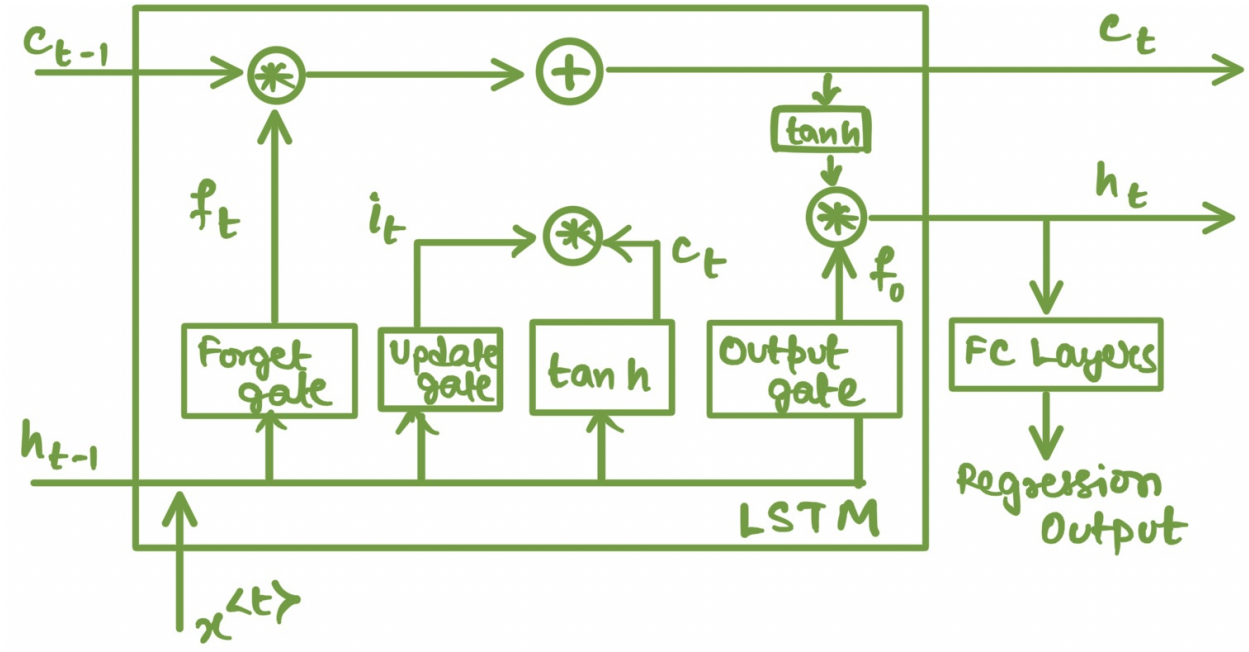

In our case we would be using LSTMs for a regression setup. But the problem arises of how to feed in the inputs to our LSTM model? Since, our data is high-dimensional i.e. the number of voxels per ROI is quite high(atleast 500, to an upper bound of over 2000).
So, we decide on using the following inputs for each subject:

- Average BOLD values(averaged across the voxel BOLDs) for each time point.
- Multivariate BOLD values for each time point(i.e. no reduction number of voxels).

Now, after deciding on the inputs, we have no prior knowledge of what model hyperparameters would suffice or perform the best compared to the others. Hence, we used several different hyperparameter combinations from the following choices:

- 1, 2 LSTM Layers
- 8, 16, 32 Hidden Units
- 1, 2, 3, 4 Dense Layers
- 0.3 Dropout Probability

Now, the model is trained using Mini-Batch Gradient Descent. We used Adam Optimizer. We trained the models on each ROI separately for 100 epochs. We used Mini-Batch size of 20. We used the Mean Squared Error loss function. 111 young subjects were split into 101 as

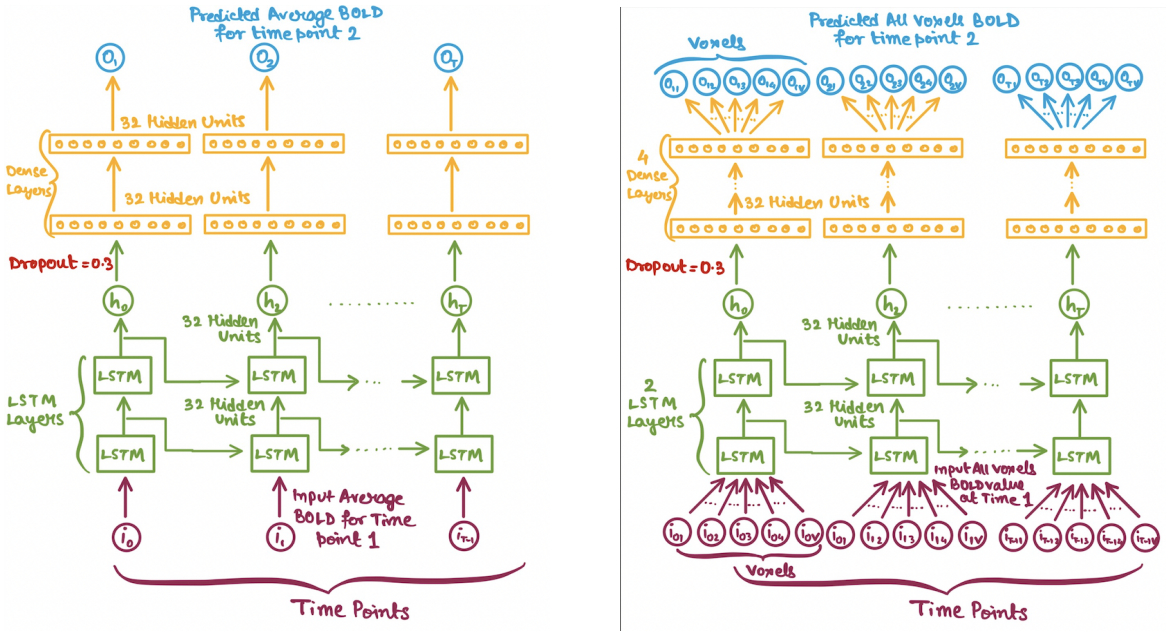

(a) Average BOLD LSTM

(b) Multivariate BOLD LSTM

Figure 3. 2 Model Architectures

training subjects and rest 10 as validation subjects. As a basic pre-processing step we used MinMaxScaling of the BOLD values, before feeding to the model. Our model is for predicting 1 TR ahead BOLD values.

RESULTS

Behavioral analysis. To prove that the older people have differential emotion perception than the Young individuals, we looked into their accuracy for the FER task for the Happy, Sad and Fear emotions. We found that for all three emotions the accuracy differed significantly between the two groups (Happy: Mean Accuracy: 98%(Y), 96%(O); $p < 0.001$; Cohen's $d = 0.5$; Sad: Mean Accuracy: 96%(Y), 83%(O); $p < 0.0001$; Cohen's $d = 0.99$; Fear: Mean Accuracy: 84%(Y), 62%(O); $p < 0.0001$, Cohen's $d = 1.13$). However, the negative emotions showed much more difference with a larger effect size.

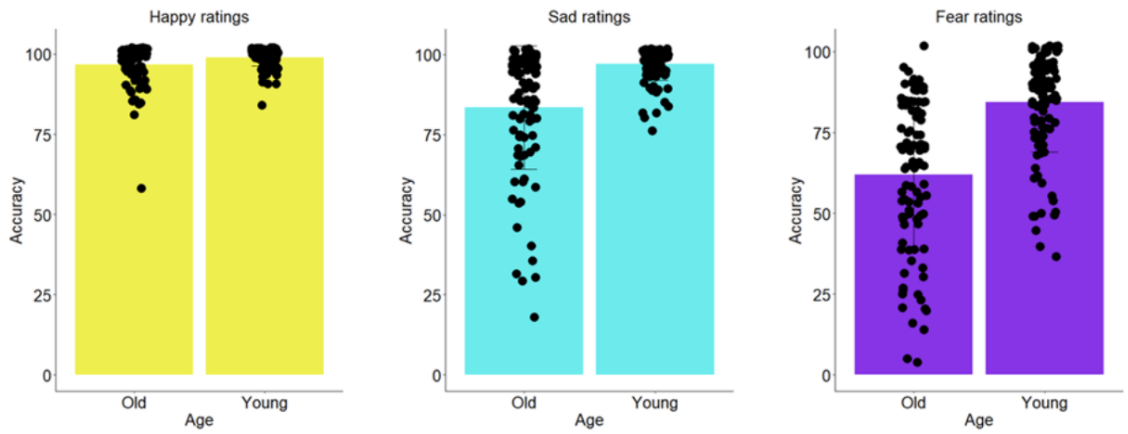

Figure 4. The figure shows the difference in Accuracy between the Old and Young groups for the Happy, Sad and Fear emotions in the FER task.

Temporal Principle Component Analysis. We employed a spatio-temporal PCA on the BOLD time series extracted from 20 ROIs (containing sensory, multi-sensory and higher order cortical areas). We found that the first two components could explain 71% of the variance in Young compared to only 57.8% variance in Old hinting on the idiosyncratic nature of their BOLD activation.

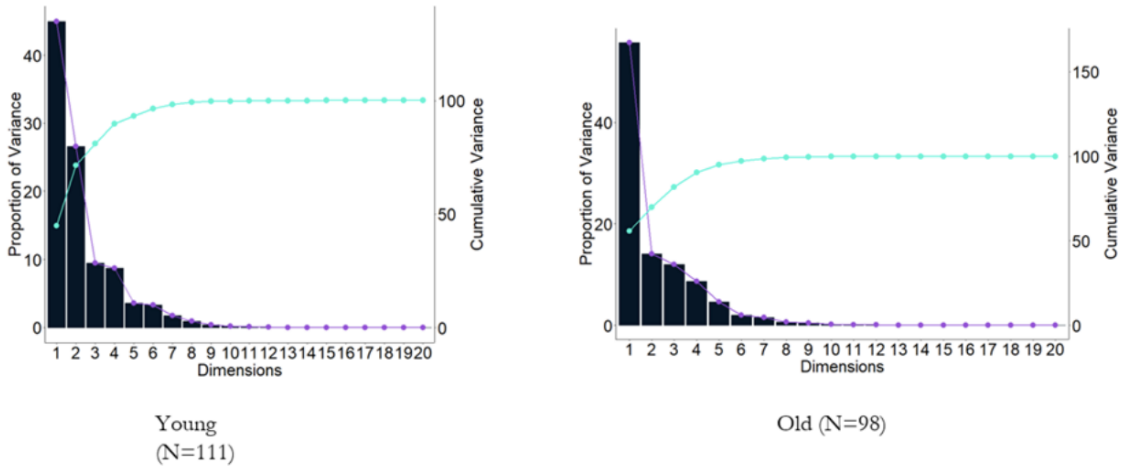

Figure 5. Scree plot for the PCA showing the cumulative and proportion of variance explained by each component for the Young and the Old

First, to assess the temporal evolution of the first 2 components, we performed a temporal PCA by computing the dot product of the PC weight vectors with the BOLD time series of the ROIs. This yielded corresponding tPCs (temporal components), which were then averaged across the subjects to obtain the group level tPCs for the Young and Old. We found that the tPC1 correlated highly with Ascent Uncertainty for the Young (r = 0.93) and Old (r = 0.76).

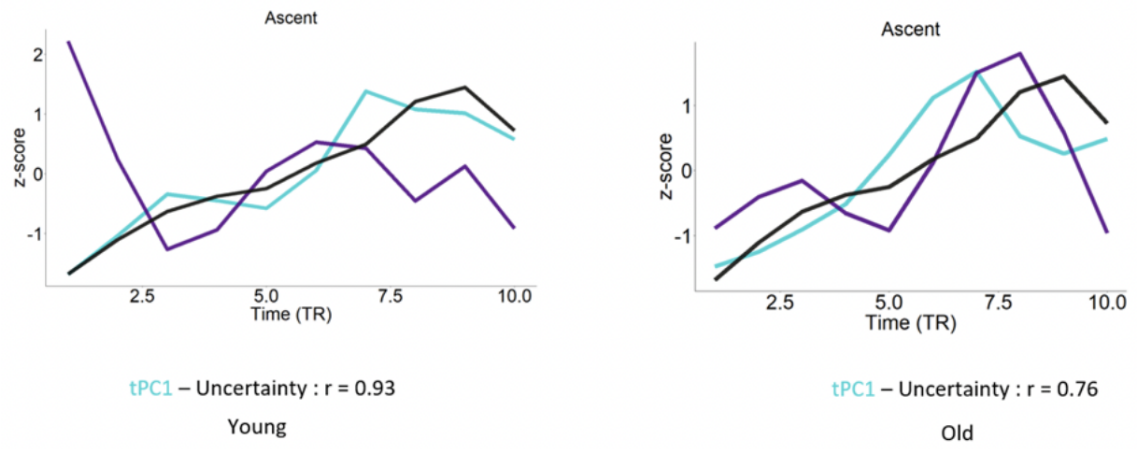

Figure 6. Temporal PCA showing the correlation of tPC1 with the Ascent Uncertainty for the two groups

Thereafter, we performed a spatial PCA on individual subject's multivariate data from the Ascent and Descent scenes to obtain the weights associated with each ROI for the first 2 components. We found that for Young this component was mainly mediated by the lateral regions of the brain while for the Old it was mainly mediated by the medial regions.

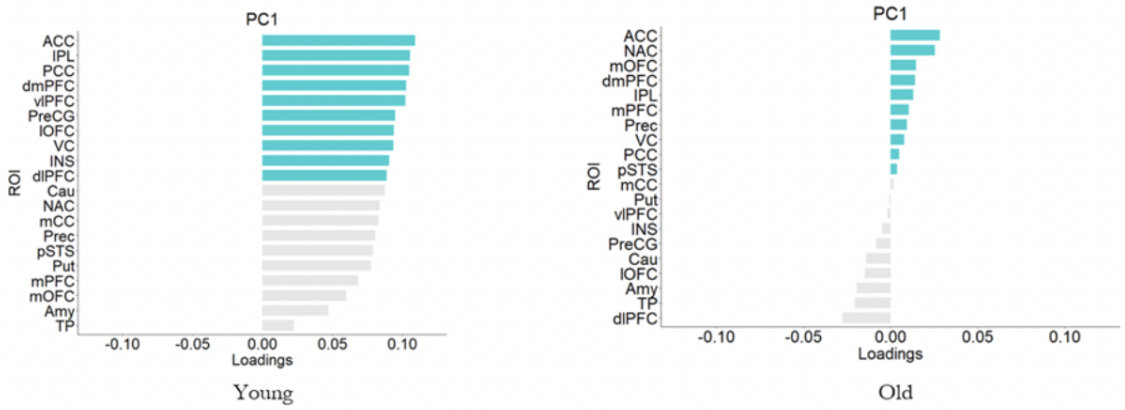

Figure 7. Spatial loadings for the PC1 for Young and Old

Temporal Potential of Heat-diffusion for Affinity-based Trajectory Embedding. A recent study showed that for complex representation architecture Temporal PHATE can capture both the global and local information of the data thus adding onto our previous result. We wanted to see whether we can find a significant difference in the low dimensional signature of the lateral and medial orbitofrontal cortex by implementing this TPHATE. The motivation for choosing these areas comes from the previous work from this lab.

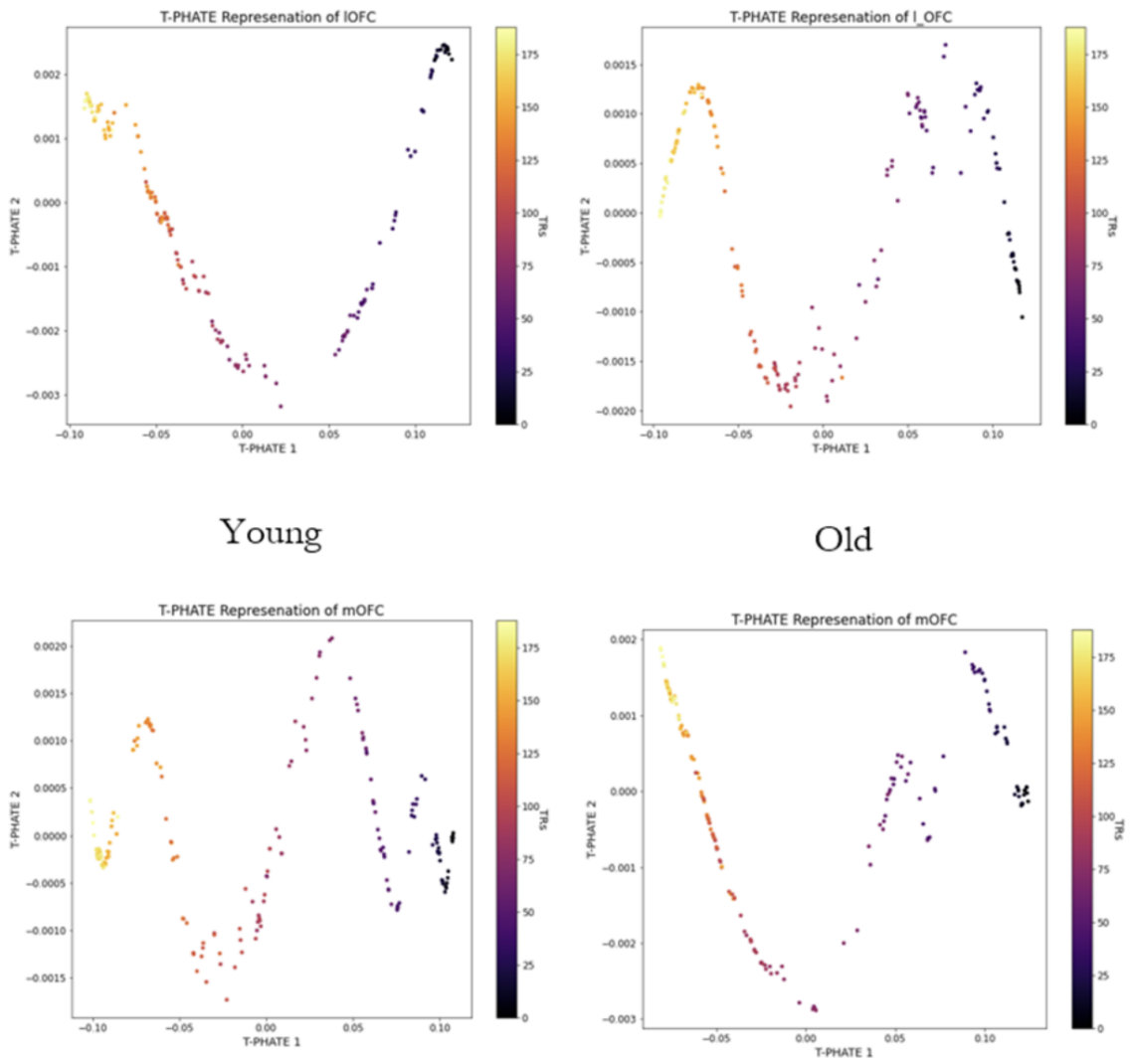

Figure 8. TPHATE on the voxel wise BOLD data of the lOFC and mOFC for the Young and the Old

Long Short-Term Memory Neural Network. As per the methodology described in the previous section, we after training the models with different sets of hyperparameters and architectures tracked the model performances based on the following criterias:

- Correlation between the actual and predicted BOLD signals for the validation subjects.
- Scaled training subjects mean squared error loss.
- Scaled validation subjects mean squared error loss.
- Validation subjects mean squared loss.
- Ascent and descent wise actual and predicted BOLD correlation for validation subjects.

We also look at the prediction plots, training loss and validation loss plots to identify any problem with the models.

Average BOLD LSTM. Here we present the predictions for mOFC and lOFC of the 8^{th} young subject for the model with 2 LSTM Layers, 32 Hidden Units in both Dense and LSTM Layers, 2 Dense Layers and 0.3 Dropout probability are shown below along with the training subjects and validation subjects loss. The correlation between the actual and predicted BOLD signals for 8^{th} young subject for mOFC is 0.88 and for lOFC is 0.87. The scaled training set MSE loss is

0.00199 and 0.00166 for mOFC and lOFC respectively whereas the scaled validation set MSE loss is 0.00157 and 0.0008 for mOFC and lOFC respectively. The pink portion indicates ascent, whereas the green portion indicates the descent.

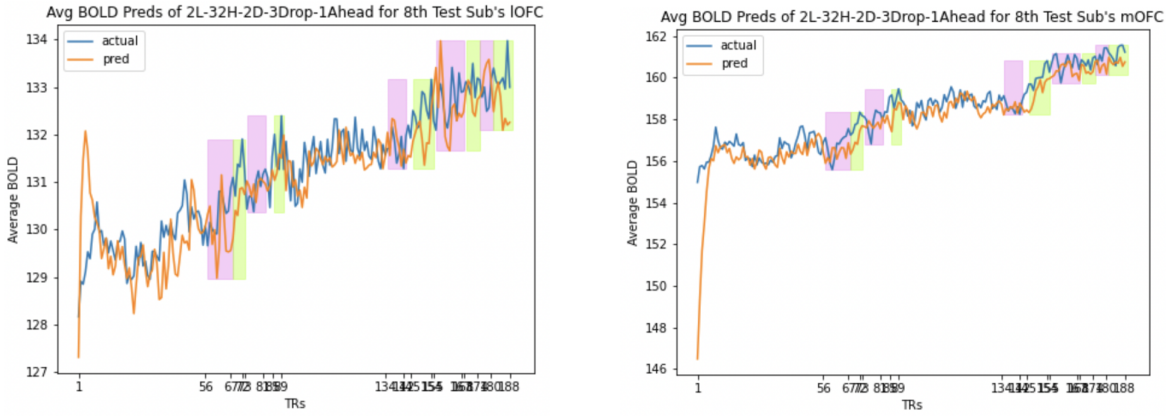

(a) lOFC (b) mOFC

Figure 9. Average BOLD LSTM Predictions

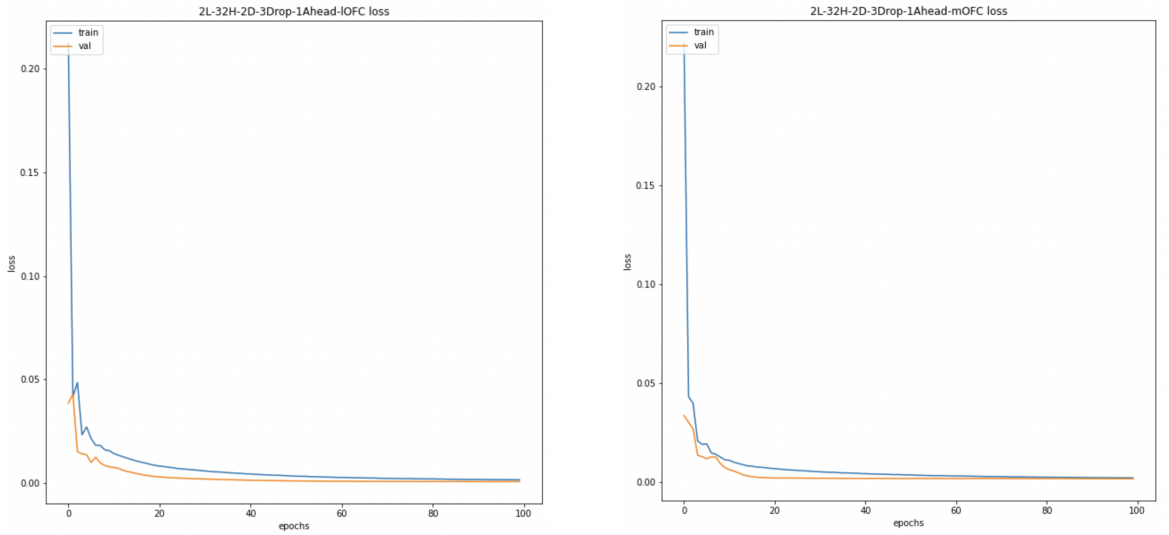

(a) lOFC (b) mOFC

Figure 10. Average BOLD LSTM Losses

Multivariate BOLD LSTM. Here we present the predictions for mOFC and lOFC of the 8^{th} young subject for the model with 1 LSTM Layers, 128 Hidden Units in LSTM Layer, 1 Dense Layers with 1 Unit and 0.3 Dropout probability are shown below along with the training subjects and validation subjects loss. The correlation between the actual and predicted BOLD signals for each voxel averaged for 8^{th} young subject of mOFC is 0.77 and of lOFC is 0.79. The scaled training set MSE loss is 0.00688 and 0.00687 for mOFC and lOFC respectively whereas the scaled validation set MSE loss is 0.00297 and 0.00399 for mOFC and lOFC respectively. The validation set MSE loss for mOFC and lOFC are 10.61 and 12.60 respectively, and the MSE loss for the 8^{th} young validation subject is 13.40 and 10.35 respectively.

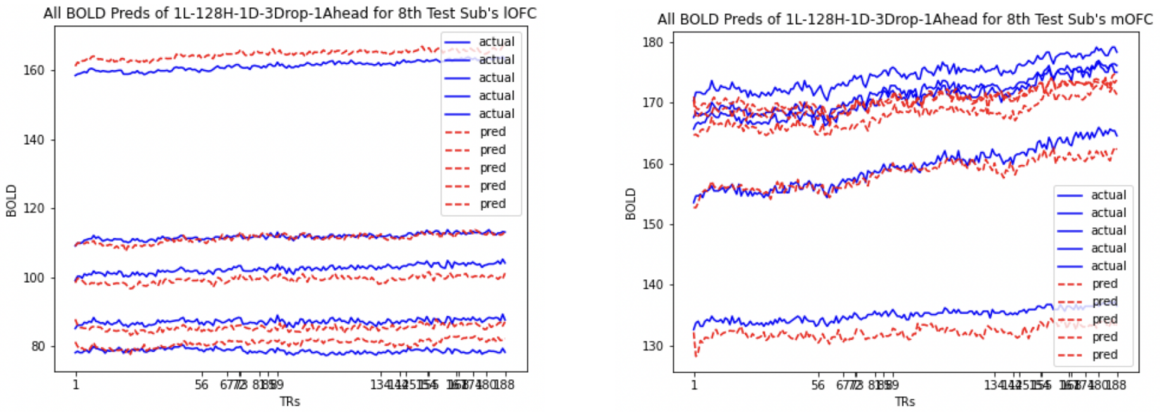

(a) lOFC (b) mOFC

Figure 11. Multivariate BOLD LSTM Predictions for 5 randomly selected voxels

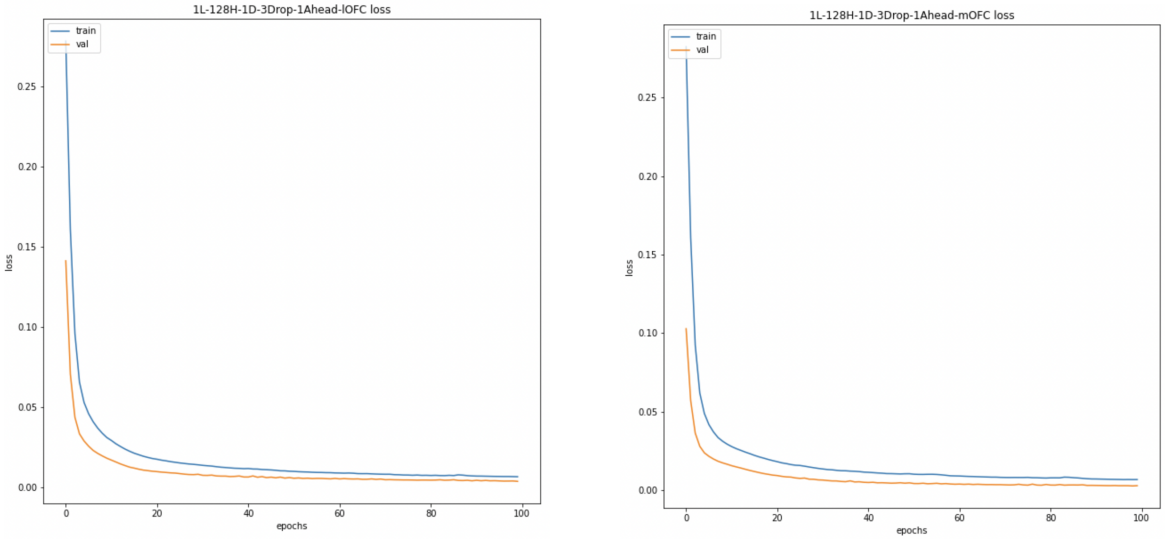

(a) lOFC (b) mOFC

Figure 12. Multivariate BOLD LSTM Losses

DISCUSSION

By analysing the neuroimaging data using multiple data unsupervised approaches, we observed that the low dimensional representation of the lOFC and mOFC completely shifts from Young to Old. Since lOFC has already been implicated in mediating the Uncertainty in Young this gives us an interesting avenue to look into future. The preliminary LSTM models gave us an few potential branches that we can follow to explore the our main question on estimating how far ahead uncertainty is estimated in Young and Old.

FUTURE WORK

There are a sequence of work lined up following this analysis. Where we will crack down concretely on the computational models and representation extracted from these computational models both quantitative and visual to represent uncertainty.

Some of the upcoming areas which we plan to extend our work to are:
1. Using low-dimensional extracted features like TPHATE along with BOLD values of voxels to see if there is significant improvement in the model being able to capture the uncertainty based information.
2. Using Masked Attention Based LSTM Model to extract parts of the BOLD time series to which the model pays most attention for BOLD value predictions of the descents.
3. The current models are trained on young subjects data, so we will be using the selected model for the old subjects to compare the results and accuracy.
4. Coming to the raised question of how far ahead the young subjects are predicting compared to the old subjects we will train the selected model for 2 TR, 3 TR, . . . , upto 15 TR ahead prediction and compare the slopes of prediction loss and correlation.
5. Using Multi-Modality of our data i.e. incorporating Movie frames information along with BOLD values for each ROIs and coming up with a uncertainty map of regions of focus in the movie as well as the ROIs responsible.
6. Devise or track other measures for model selection as well as quantify uncertainty based on metrics for similarity and distance between actual and predicted signals.
7. Reduced Voxel Dimensionality using unsupervised methods to extract maximum relevant information.

FUTURE WORK CONTD.

3. The current models are trained on young subject's data, so we will be using the selected model for the old subjects to compare the results and accuracy.

4. Coming to the raised question of how far ahead the young subjects are predicting compared to the old subjects we will train the selected model for 2 TR, 3 TR, . . . , upto 15 TR ahead prediction and compare the slopes of prediction loss and correlation.

WORK:

I modelled the BOLD values up to 15 TRs ahead for both young and old subjects. Below, I present the plots of prediction error and correlation of predicted BOLD values with the actual BOLD values for all these models for predicting BOLD values ahead of time. I only show the models for mOFC and lOFC. The other plots can be found here.

- We have around 10 test subjects, and we have individual results for each of them. Here I present the averaged result across all these subjects.
-

PREDICTION ERRORS:

- **mOFC**

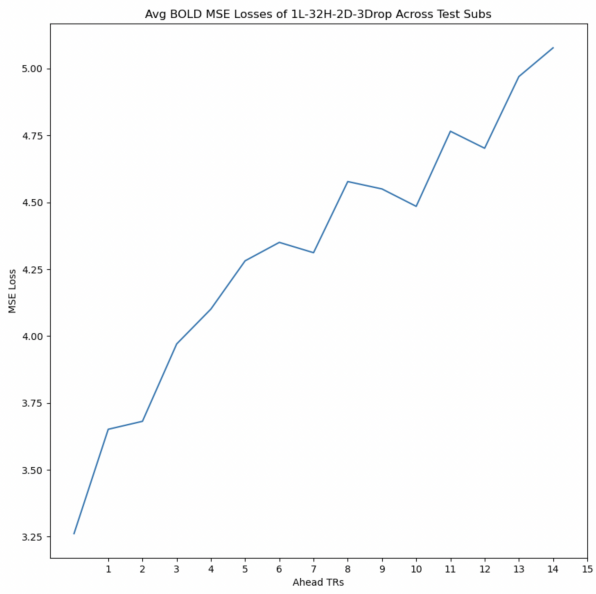

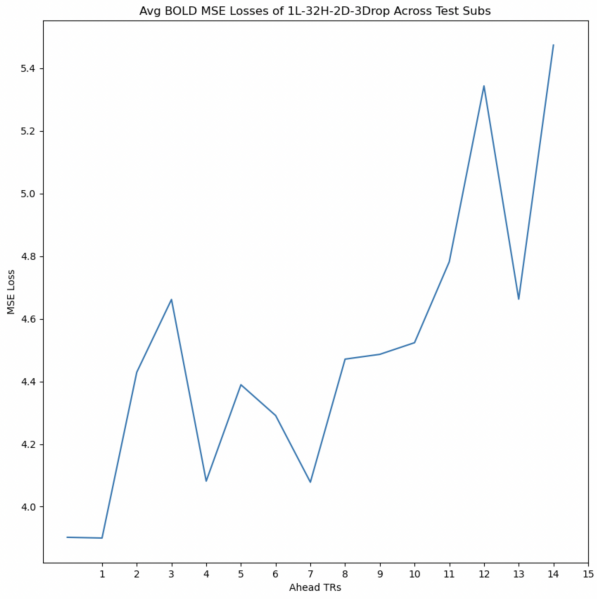

YOUNG

OLD

As expected, the loss increases as the time point ahead where the BOLD value is predicted increases. But the loss values for the OLD subjects are higher than the YOUNG subjects.

- **lOFC**

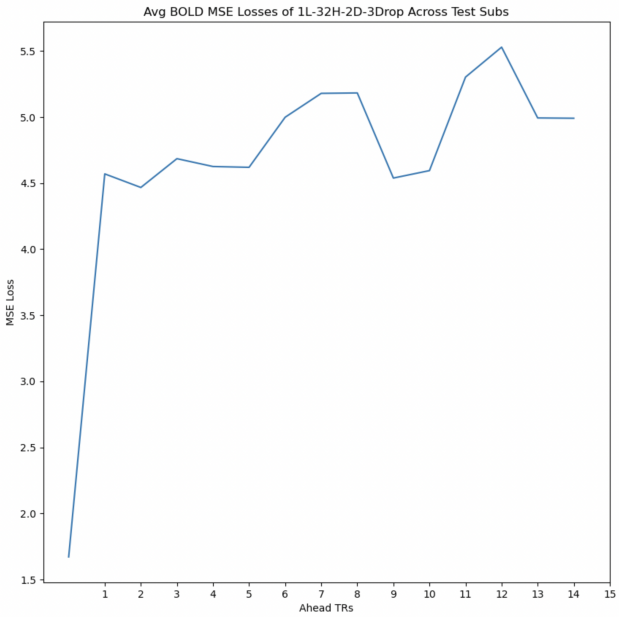

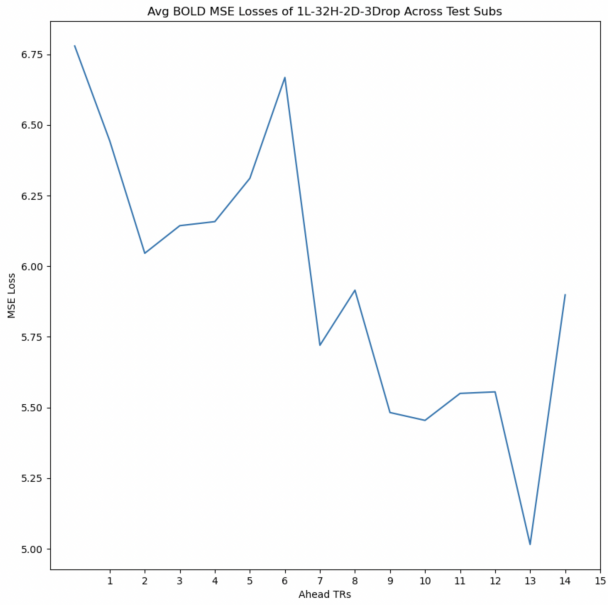

YOUNG OLD

Looking at the Y-axis you can see the error values are higher in old subjects like before. But the stark difference is prediction loss actually decreases as the time ahead when the BOLD values are predicted increases for the old subjects.

CORRELATION:

- **mOFC**

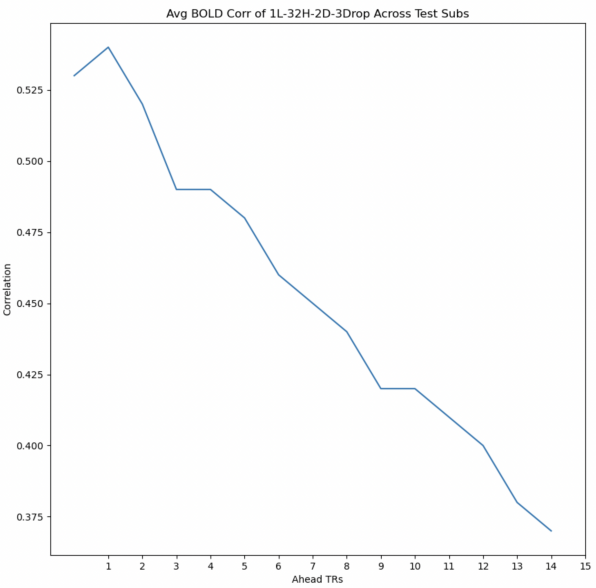

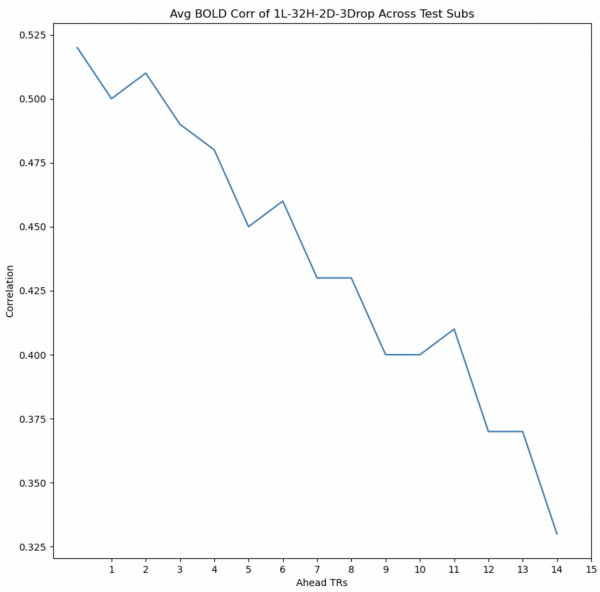

YOUNG OLD

- **lOFC**

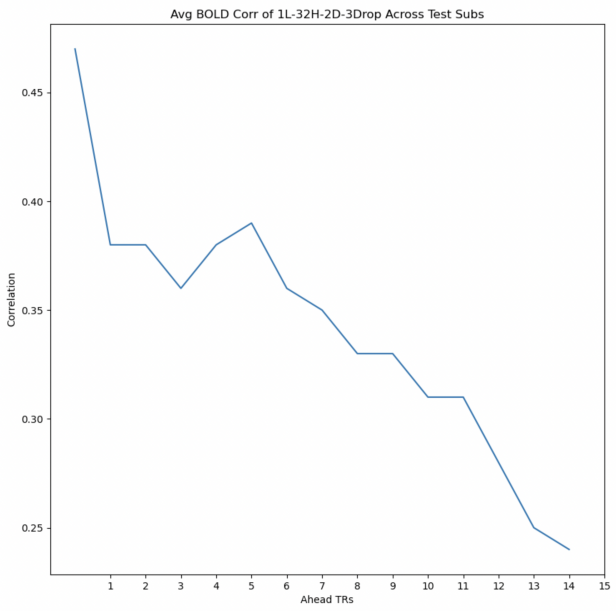

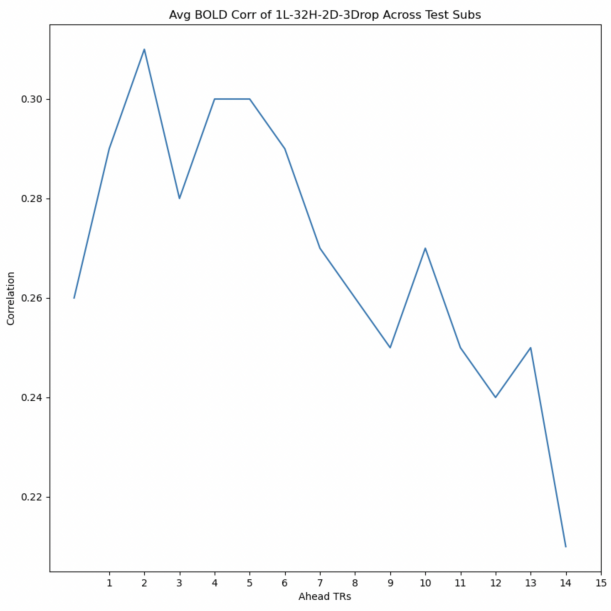

YOUNG OLD

The correlation drops as the time ahead when predictions are made increases in both young and old subjects.
But common observations from the plots for old subjects are more erratic compared to young subjects.

6. Devise or track other measures for model selection as well as quantify uncertainty based on metrics for similarity and distance between actual and predicted signals.

Trying to attack in this direction, I estimate the entropy throughout the movie from the 1 TR ahead prediction model. Below, I present the results.

- **mOFC**

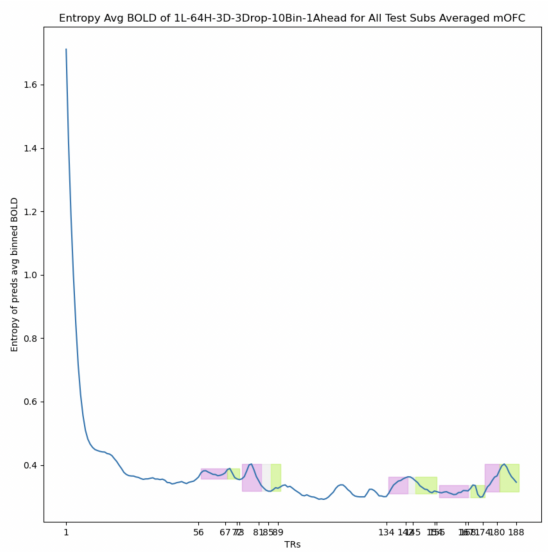

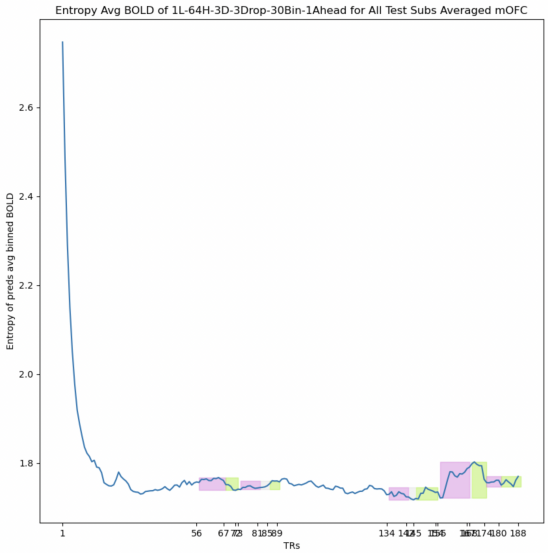

YOUNG OLD

- **IOFC**

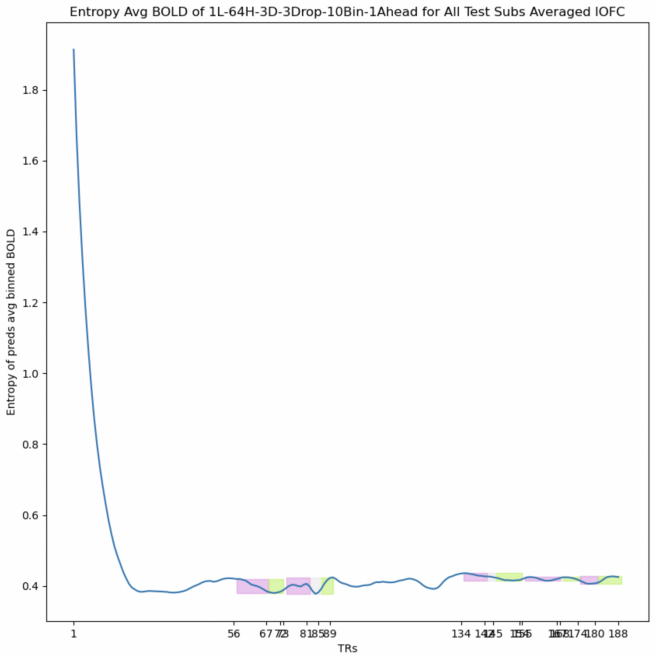

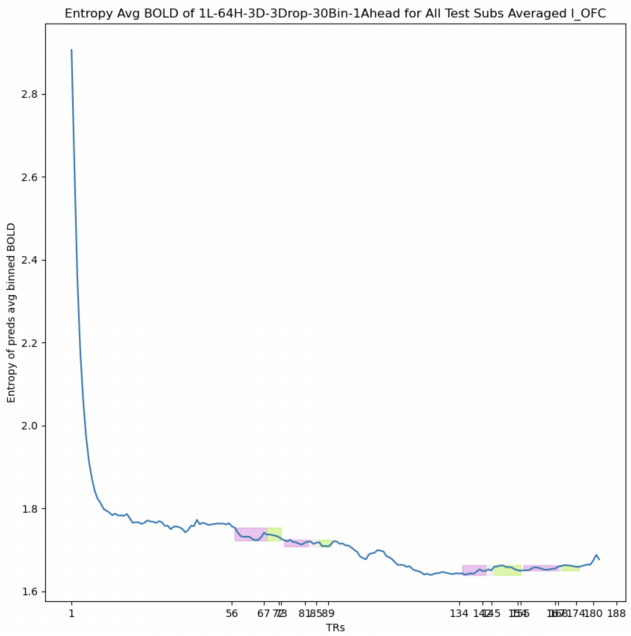

YOUNG OLD

The entropy values on the Y-axis for young subjects are lesser than for old subjects. But the entropy values for older subjects are more jittery compared to the young subjects.